JOURNAL OF APPLIED ELECTROCHEMISTRY **27** (1997) 1275–1282

Carbon monoxide electrooxidation on porous Pt–Ru electrodes in sulphuric acid

A. S. ARICÒ, E. MODICA, E. PASSALACQUA, V. ANTONUCCI

CNR Institute for Transformation and Storage of Energy, Salita S. Lucia sopra Contesse 39, 98126 S. Lucia, Messina, Italy

P. L. ANTONUCCI

University of Reggio Calabria, Faculty of Engineering, Institute of Chemistry, via Cuzzocrea 48, 89100 Reggio Calabria, Italy

Received 30 January 1997; revised 24 March 1997

CO electrooxidation on a Pt–Ru/C catalyst was investigated in sulphuric acid electrolyte. The physico-chemical properties of the Pt–Ru/C catalyst were studied by X-ray diffraction (XRD) and X-ray photoelectron spectroscopy (XPS). The influence of temperature, CO partial pressure and proton concentration on the electrochemical oxidation rate was investigated by steady-state galvanostatic polarization measurements. The apparent activation energy decreased from 70 to 30 kJ mol^{-1} as the overpotential increased from 0.5 to 0.9 V vs NHE. The reaction order with respect to carbon monoxide increased, passing from 0.4 to 1, with the increase of the overpotential from 0.5 to 0.7 V vs NHE; a reaction order close to -1 with respect to the protonic concentration was observed, irrespective of the potential. Tafel slopes of about 136 mV dec^{-1} were determined for oxidation of CO and CO/N_2 mixtures.

Keywords: *Carbon monoxide, Pt-Ru/C catalyst, Tafel slopes, oxidation*

1. Introduction

CO electrooxidation is a major item in the electrochemical conversion of hydrogen-rich carbon based fuels for energy purposes. As is well known, CO acts as a strong deactivating agent for the anode electrocatalyst in low temperature fuel cells [1–5]. This reaction has been widely investigated on porous gas-diffusion electrodes composed of carbon supported Pt catalyst especially in relation to the CO poisoning of phosphoric acid fuel cell anodes [6–15]. Dhar and coworkers [13, 15] observed that the anodic overpotential increased linearly with $\ln(CO/H_2)$ at low current densities in phosphoric acid. The same authors [15] have also determined the activation energy for the oxidation of various CO/H_2 mixtures on porous Pt/C electrodes in H_3PO_4 at temperatures above 110 °C.

Encouraging catalytic performance has been recently reported for Pt–Ru alloy-based electrodes in the electro-oxidation of H_2/CO mixtures [16, 17]. In contrast to pure Pt, these binary catalysts appear to facilitate the reaction path through the nucleation of oxygen-containing species on the alloying component at low potentials, therefore promoting the oxidation of adsorbed CO, according to a widely accepted bifunctional mechanism [18]. All these fundamental studies, carried out on well defined Pt–Ru surfaces (bare electrodes) have led to a good understanding of the elementary steps of the process occurring on the catalyst material. On the basis of the previous results, it was considered of interest to investigate the CO electrooxidation process using carbon supported Pt–Ru gas diffusion electrodes of the type commonly employed in low-temperature fuel cells.

A significant complexity encountered in studying electrode kinetics at porous electrodes concerns the evaluation of diffusion and ohmic overpotentials [19]. These are, in fact, so strictly connected with electron transfer kinetics to make the deconvolution of the electrode polarization into its components difficult. Gas-diffusion electrodes based on carbon black supported Pt or Pt-alloy catalysts consist of a distribution of pores with different radii (micro- and macropores) and shapes, often interconnected and with a significant degree of tortuosity. Although various physical models have been proposed, which take into account the wetting characteristics of the catalytic layer [20–24], the penetration of current inside electrode pores is not yet well known under real operating conditions. For electrodes with partial wetting behaviour two cases are mainly considered [25]. In the first case, a thin film extends out above the meniscus at the electrode–electrolyte interface and maintains a constant thickness over the catalyst; in the second case there is a finite contact angle. Recently, a.c. impedance studies of oxygen reduction at PTFE-bonded gas-diffusion electrodes in sulphuric acid have shown that the electrochemical data may be

0021-891X

suitably fitted by the thin film model of porous electrodes [26]. In the case of the thin film electrolyte there is a relative uniformity of current inside the pores even at high current densities [25]. The concentration gradient of electroactive species between the film–gas interface and the catalyst sites is governed by both diffusion coefficient of the reactant and thickness of the film within the pores as well as by Tafel kinetics. Notwithstanding the above difficulties, derivation of electrode-kinetic parameters for high surface area catalysts is of fundamental importance since, small Pt or Pt-based alloy particles, having a significant fraction of surface atoms behave differently from bulk materials. Furthermore, application of a.c.-impedance analysis to electrode polarization allows the determination of the ionic resistance within the pores [26], hence, the ohmic overpotential can be evaluated at the various current densities. Besides, an evaluation of the contribution of mass-transport to the electrode polarization could be made by digital simulation of current-potential data [27]. Thus, the aim of this study was to understand to what extent the results obtained for CO oxidation on smooth electrodes were also valid for dispersed Pt–Ru particles supported on carbon.

2. Experimental details

A 20%Pt–10%Ru catalyst supported on a high surface area, conductive carbon black (Vulcan XC72) was purchased from Electrochem. Inc. (Woburn, MA). XRD analysis was carried out with a Philips X-Pert diffractometer using a CuK_α source. The XPS measurements were performed using a VSW Scientific Instruments spectrometer (Manchester, England); X-ray source was AlK_α operating at a power of 150 W. The samples were introduced into the spectrometer using a separate differentially pumped fast entry chamber, then into desorption chamber in ultrahigh vacuum for desorption of high volatile species adsorbed on carbon support, and finally into the analyser chamber.

Porous electrodes comprised a Teflon™-bonded Pt–Ru catalyst layer deposited onto a wet-proofed carbon paper acting as diffusion layer. The electrodes were prepared by first mixing the catalyst powder with water at 60 °C in an ultrasonic bath. Subsequently, a suspension of polytetrafluoroethylene (PTFE) was added to the catalyst up to obtain a 40% PTFE loading in the catalytic layer. The as-obtained paste was spread by doctor-blade technique over a Toray carbon paper (Toray TGP 90) wet-proofed with a solution of fluoroethylenepropylene polymer (FEP T120, DuPont). The electrode was pressed at 70 °C under 15 kg cm^{-2} for 30 min, then treated in air at 350 °C for 25 min. The platinum loading in the electrodes was 0.5 mg cm^{-2}.

Electrochemical measurements for the electrooxidation of carbon monoxide and CO/N_2 mixtures were carried out at various H_2SO_4 concentrations (0.5, 1, 2.5, 4 M). The apparatus consisted of a water-thermostated three-electrode cell. The gas diffusion electrode was mounted into a Teflon holder containing a Pt ring current collector. The electrode area exposed to the electrolyte was 0.5 cm^2. A large area Pt gauze was used as counter electrode. An AMEL saturated calomel reference electrode (SCE) was placed in an external compartment filled with the same electrolyte and connected to the main body with a Luggin capillary whose tip was placed appropriately close to the working electrode. Electrode potentials in the text were reported with respect to the normal hydrogen electrode (NHE). The electrochemical cell was connected to an EG&G PAR model 273-A potentiostat/galvanostat and a Solartron 1255 frequency response analyser. Series resistance values were obtained from a.c. experiments.

3. Results

3.1. *X-ray diffraction analysis*

The X-ray diffraction pattern of 20%Pt–10%Ru/C catalyst is shown in Fig. 1. The catalyst exhibits the diffraction peaks of the Pt f.c.c. structure (JCPDS 4-802) and the C(0 0 2) reflection of graphitic carbon black. A lattice parameter of 390.5 pm was determined by least-squares fitting of the (2 2 0) reflection (see inset in Fig. 1) which accounts for the presence of a Pt–Ru solid solution.

The average particle size of the catalyst was determined from the broadening of the (2 2 0) reflection by using the Debye–Scherrer equation. The full width at half maximum (FWHM) value was corrected for the instrumental broadening by using the Warren formula. A mean particle size of 3.8 nm was determined for the Pt–Ru particles in the catalyst.

3.2. *XPS analysis*

The XP spectra of the Pt–Ru catalyst are shown in Fig. 2(a)–(c). The C 1s signal (Fig. 2(a)) from carbon support at about 284.6 eV overlaps to Ru $3d_{3/2}$ (284 eV) peak, averting the investigation of oxidized Ru species in this spectrum.

More detailed information is obtained by the investigation of Ru $3p_{3/2}$ signal (Fig. 2(b)). This latter derives from the contribution of two components with binding energy of 463.37 and 466.90 eV having 84% and 16% relative intensities, respectively; such peaks could be attributed to RuO_2 and RuO_3 species [28]. Yet, the large width ($\sim$ 4 eV) of the main peak would suggest that it derives from the convolution of two species with similar binding energies [29], associated with RuO_2 species and Ru atoms in the alloy.

The Pt 4f signal for the Pt–Ru/C sample is shown in Fig. 2(c). To achieve a consistent fit of the spectral data, three components were needed for the Pt $4f_{7/2}$ at binding energies 71.78 (Pt^0), 73.20 (Pt^{II}) and 74.65 eV (Pt^{IV}) [30, 31]. The oxidized Pt(II) and Pt(IV) species (Fig. 2(c)) show a significantly lower relative intensity with respect to zero valent Pt.

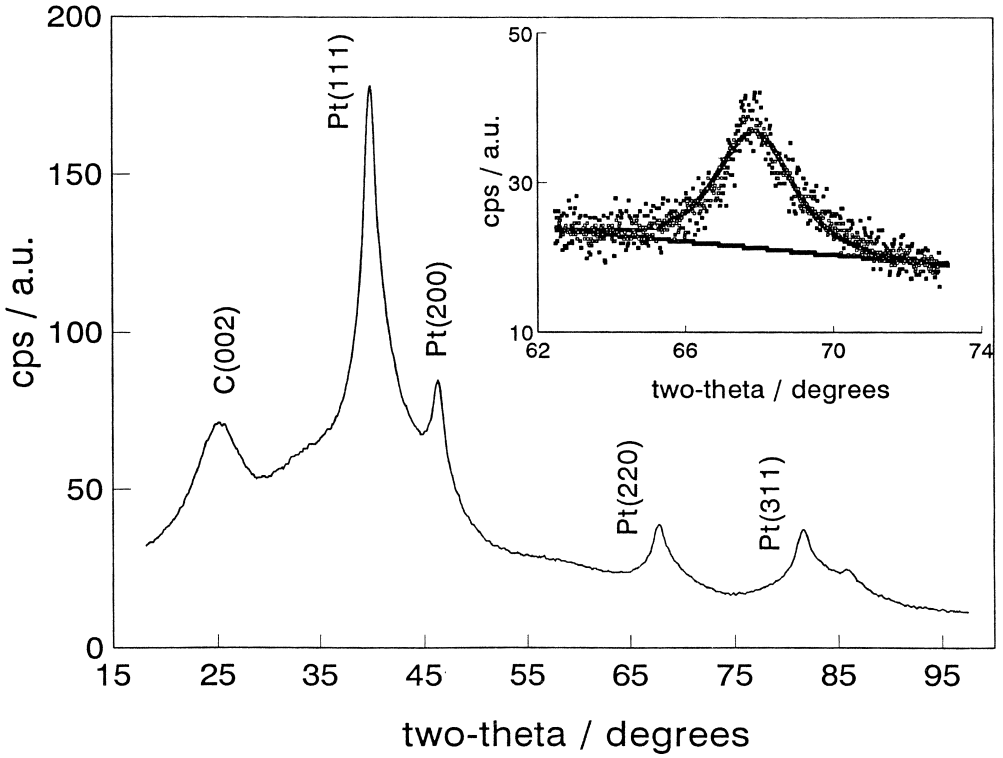

Fig. 1. X-ray diffraction pattern of carbon supported Pt–Ru catalyst. C indicates the graphitic carbon. The inset shows the Pt–Ru (2 2 0) peak profile fitting.

3.3. *Electrochemical polarization experiments*

Figure 3 shows the steady state galvanostatic polarization for 50 kPa CO at 70 °C for different H_2SO_4 concentrations (0.5, 1, 2.5, 4 M). The shape of the curves denotes strong activation control at low current densities, afterwards mixed ohmic losses and mass transfer limitations influence the polarization behaviour [27]. An increase in the electrolyte concentration negatively affects the electrocatalytic performance, consistently with the hydrogen ions release in the electro-oxidation of methanol. Furthermore, as the concentration of sulphuric acid increases, the sulphate ions compete with water dipoles for the electrostatic adsorption on the electrode surface. This effect may depress the water discharging reaction which is involved in the oxidation of adsorbed CO species. The series resistance values (R_u) were obtained from a.c. experiments by the high frequency intercept on the real axis of the Nyquist plot [32]. The observed values vary significantly with the electrolyte concentration, decreasing from $0.35\,\Omega\,cm^2$ to $0.2\,\Omega\,cm^2$ as the sulphuric acid concentration increases from 0.5 to 4 M, and they increase only slightly with the current density ($< 0.03\,\Omega\,cm^2$). Series resistance values were employed for the correction of ohmic drop effects in the derivation of electrode-kinetic parameters. No significant evidence of Ru dissolution during electrode polarizations is observed in the absence of CO, even when the positive potential limit is above 0.75 V vs NHE (see inset in Fig. 3).

The temperature-activated nature of the reaction is denoted in Fig. 4, where higher overpotentials are recorded as temperature decreases from 70 to 40 °C. Figure 5 shows the Arrhenius plots at potentials varying between 0.5 and 0.9 V vs NHE. Activation energies (E_a) [15] in the range 30–70 kJ mol^{-1} for 50 kPa CO are observed. As shown in Fig. 6, a nearly two-fold decrease in E_a is observed passing from 0.5 to 0.9 V vs NHE. This is thought to be connected with a significant potential activation of the rate-determining step (r.d.s.); besides, the formation of a suitable coverage for the species involved in the r.d.s. could be strongly dependent on the potential. At low overpotentials, the water discharging is impeded due to the large affinity of the catalyst surface towards CO adsorption (~ 120 kJ mol^{-1}) [33], whereas at high overpotentials (0.9 V vs NHE) formation of platinum oxide can hinder the strong adsorption of carbon monoxide at Pt.

3.4. *Effect of CO partial pressure on the electrooxidation process*

Figure 7 shows the polarization curves obtained at different CO partial pressures (5, 10, 50, 100 kPa). At low current densities the overpotential decreases passing from 5 to 50 kPa CO, then it increased again passing from 50 to 100 kPa CO. At current densities above 50 mA cm^{-2} the performance of the polarization curve in presence of 10 kPa CO is better than in 100 kPa CO, although mass transfer limitations are observed above 200 mA cm^{-2} in the first case. The results suggest that the increase of CO coverage on the electrode surface with the increase in partial pressure produces a significant increase of the reaction rate, yet, this reaches a maximum for the 50 kPa CO in N_2 mixture, after that a decrease is observed

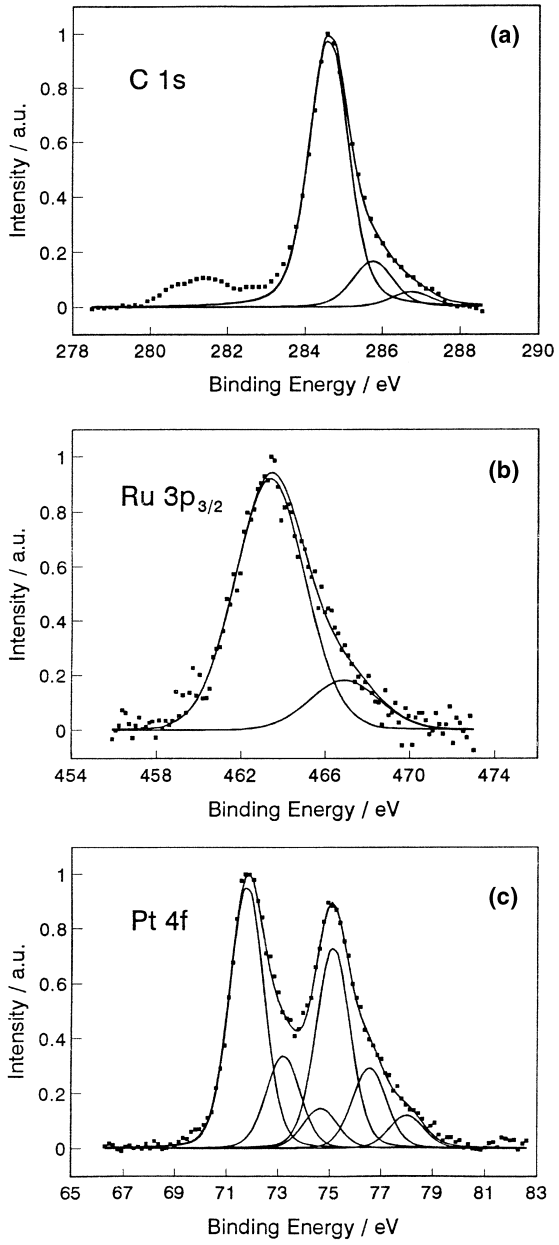

Fig. 2. X-ray photoelectron spectra of the Pt–Ru/C catalyst. The experimental spectra are shown by dots and the fitted spectra by lines.

for 100 kPa CO. It appears that a large coverage of catalyst sites by strongly adsorbed CO could hinder the water discharging process that produces OH_{ads} species participating to the bimolecular reaction. Carbon monoxide is strongly adsorbed on both Pt and Ru sites [16, 17], thus a competition between CO and water molecules for these sites is established.

3.5. *Tafel analysis*

The variation of current density (I) with potential (E) for an irreversible anodic process is described by the following equation [34]:

$$E = E_{rev} - \frac{RT}{\alpha n_a F} \ln \frac{I_o(I_L - I)}{II_L} + IR_u \qquad (1)$$

where I_o is the exchange current density, E_{rev} is the reversible potential, n_a is the number of electrons involved in the rate-determining step, α is the anodic charge transfer coefficient. I_L is the diffusion limiting current, the other parameters have the usual meaning. I_L values were obtained by an analytical least-square regression procedure [27]. Series resistance values were determined by the a.c. impedance method. Figures 8 and 9 show the ohmic drop and mass transfer corrected Tafel plots [27] for the oxidation of CO at two different partial pressures and proton concentrations, respectively. A single Tafel region is observed, which extends over almost three decades of current density. It is interesting to note that the Tafel slope (β) in all the cases is close to $\left(\frac{2.3\,RT}{0.5\,F}\right)$ or $136\,mV\,dec^{-1}$ at 70 °C, which could account for a single electron transfer in the r.d.s.

3.6. *Electrochemical rate equation for CO oxidation on Pt–Ru/C catalyst*

The previous results indicate that the reaction rate for the electrooxidation of carbon monoxide is strongly dependent on CO partial pressure and protonic concentration, besides electrode potential and reaction temperature. Accordingly, the reaction rate (r) could be mathematically expressed as follows:

$$r = k P_{CO}^{\gamma} C_{H^+}^{\delta} \exp(\alpha n_a F \eta / RT) \qquad (2)$$

where k is the intrinsic reaction rate, η is the overpotential ($\eta = E - E_{rev}$), P_{CO} is the CO partial pressure and C_H^+ the proton concentration.

The reaction orders with respect to CO (γ) and H^+ (δ), at various potentials, can be determined from the ohmic drop-corrected polarization curves by plotting $\ln I$ against $\ln P_{CO}$ and $\ln I$ against $\ln C_H^+$, respectively; these plots are shown in Figs 10 and 11, respectively. A suitable linear trend is observed only in the range from 5 to 50 kPa CO in N_2 and at potentials lower or equal to 0.7 V vs NHE (Fig. 10). The slope of $\ln I$ against $\ln P_{CO}$ increases with the overpotential, passing from about 0.4 at 0.5 V to 0.5 at 0.6 V and to 1 at 0.7 V vs NHE. The mass-transfer overpotential, i.e., $\eta_{conc} = -(RT/nF)\ln(1 - (I/I_L))$ [35], is estimated to be less than 20 mV in the range of current densities reported in the plots of Figs 10 and 11 at potentials below 0.7 V vs NHE. The influence of concentration polarization on the reaction order is considered to be less than 10% of the estimated value. From 50 to 100 kPa CO partial pressure a decrease of reaction rate is observed (Fig. 10), indicating a negative reaction order probably due to a partial blocking effect of Ru sites for water displacement [36]. A similar analysis is carried out for proton concentration. The reaction order with respect to $[H^+]$ was determined from plots of $\ln I$ against $\ln[H^+]$ in the potential range from 0.5 to 0.9 V vs NHE; a value close to -1 is found, irrespective of the potential (Fig. 11).

The variation of oxidation current as a function of CO partial pressure (range 5–50 kPa CO) and proton concentration was analysed with respect to Langmuir and Temkin relationships [37–39]. The best fit of

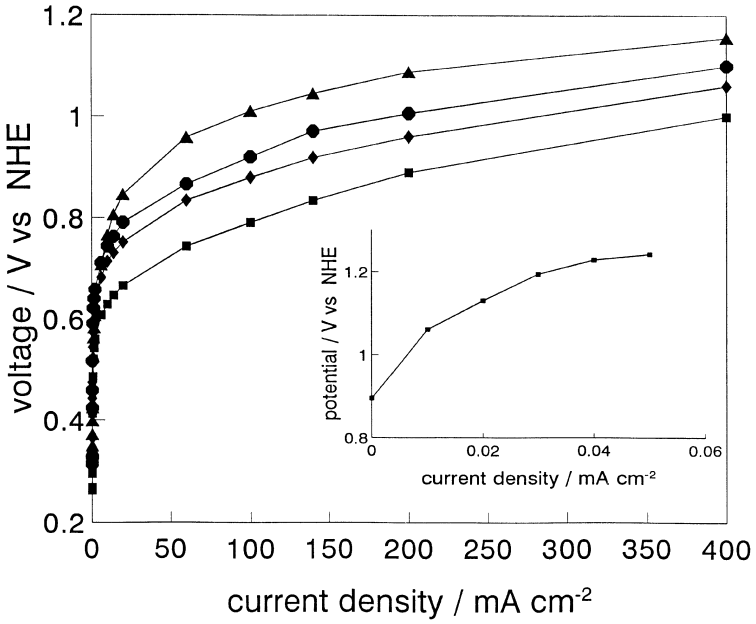

Fig. 3. Galvanostatic polarization curves for carbon monoxide (50 kPa) oxidation at 70 °C on Pt–Ru/C electrode at various concentrations of H_2SO_4. The inset shows the polarization data of Pt–Ru/C in absence of CO in 0.5 M H_2SO_4. Concentrations: (■) 0.5, (◆) 1.0, (●) 2.5 and (▲) 4.0 M.

experimental data is observed in the Temkin diagram (Fig. 12), suggesting that the adsorption energy decreases as a function of the coverage of electrode surface by CO and OH species. In a previous paper, Dhar *et al.* [15] observed that the CO adsorption on porous Pt electrodes in phosphoric acid was governed by the Temkin adsorption isotherm. The fact that a suitable Temkin relationship is observed for CO partial pressures between 5 and 50 kPa suggests that, under these conditions, the CO coverage does not reach the complete monolayer.

4. Discussion

The electrochemical oxidation of CO on bare Pt and Pt alloy electrodes has been widely investigated in literature [3–6, 16, 17]. *In situ* FTIR spectroscopic analyses in combination with electrochemical measurements have allowed to identify the reaction intermediates on the electrode surface [40–43]. The results obtained on porous electrodes are substantially in agreement with those reported in literature for bare electrodes. Yet, a few aspects need a more in depth analysis. At low overpotentials, the availability of OH species influences more significantly the reaction rate than the CO adsorption strength. In fact, the reaction orders with respect to CO and H^+ are +0.4 and −1, respectively, at 0.5 V vs NHE. However, the rate of CO oxidation is directly related to both coverages of CO and OH species; this is consistent with a

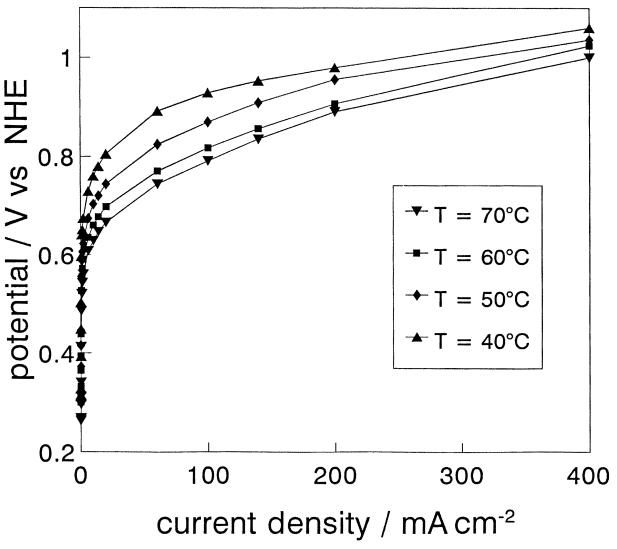

Fig. 4. Galvanostatic polarization curves for carbon monoxide (50 kPa) oxidation on Pt–Ru/C electrode at various temperatures in 0.5 M H_2SO_4.

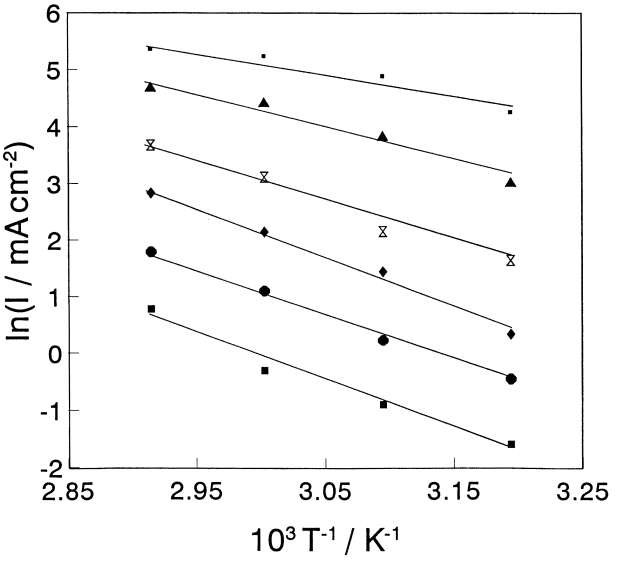

Fig. 5. Arrhenius diagram for the oxidation of 50 kPa CO in N_2 mixture on the Pt–Ru/C electrode at various potentials in 0.5 M H_2SO_4. Potentials: (■) 0.5, (●) 0.6, (◆) 0.65, (⊠) 0.7, (▲) 0.8 and (■) 0.9 V vs NHE.

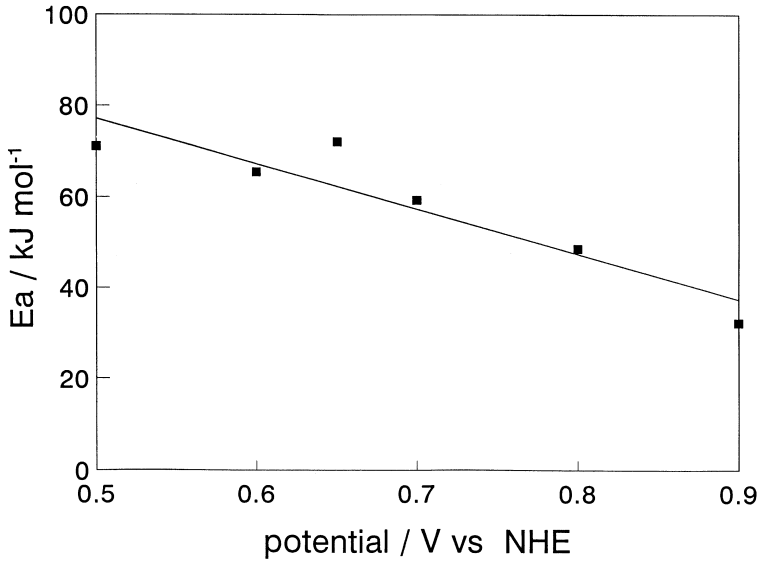

Fig. 6. Variation of the activation energy with the electrode potential for the oxidation of 50 kPa CO in N_2 mixture on Pt–Ru/C electrode in 0.5 M H_2SO_4.

r.d.s. involving a surface reaction of adsorbed CO and OH molecules.

Recently, Gasteiger *et al.* [36] have observed a cathodic shift of the onset of CO oxidation with P_{CO} on a smooth Pt–Ru surface and, thus, a negative reaction order with respect to CO at low electrode potentials (< 0.45 V vs RHE). A decrease of current density with CO partial pressure is observed, in the present case, in the range between 50 and 100 kPa CO at higher overpotentials (> 0.5 V vs NHE). The transition point, that is, the value of P_{CO} at which the reaction order changes from positive to negative, is found to shift as the potential decreases below 0.5 V vs NHE. Unfortunately, no clear estimation of reaction order is possible from the data collected at very low overpotentials on carbon supported Pt–Ru/C catalyst. A transition from a poisoned to a highly active surface with the potential was observed by Gasteiger and coworkers [17, 36] on both Pt and Pt–Ru bare electrodes. Accordingly, a modification of the reaction order at higher potentials would be expected in the same range of CO partial pressures.

XPS analysis has revealed the presence of RuO_x species, besides Pt–Ru alloy, in our catalysts. The formation of labile oxygen species especially on Ru(IV) sites, being in close proximity to Pt-rich region in the catalyst, can allow the chemical interaction between these groups and the CO species adsorbed onto Pt sites; the Ru oxide species are hence regenerated by water discharging on free Ru sites [44]. It was suggested in the literature that the oxygen transfer mechanism would better operate on an open Ru oxyhydroxide structure having a significant number of labile Ru–OH species [44]. Besides, the high mobility of adsorbed CO species on Pt sites [5] could facilitate the migration of CO towards Ru-oxide species. This reaction path can occur in parallel to the surface reaction on Pt–Ru pairs in the f.c.c. alloy.

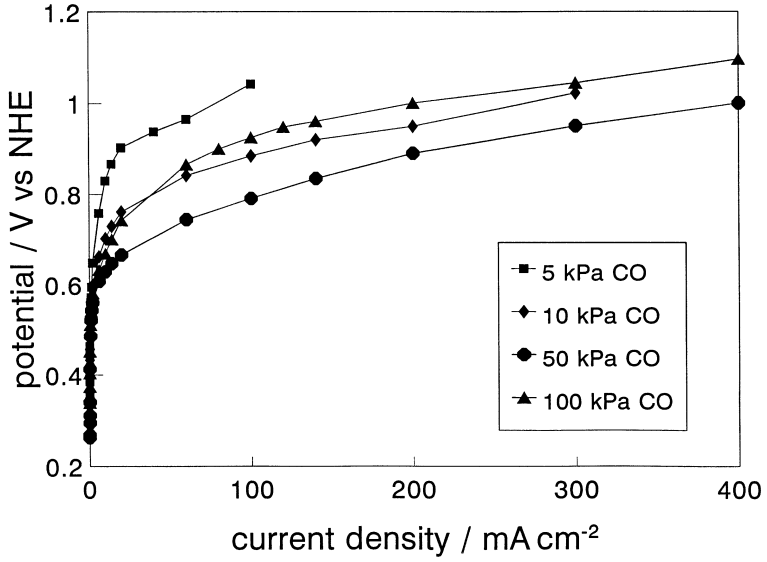

Fig. 7. Galvanostatic polarization curves for carbon monoxide oxidation at 70 °C on Pt–Ru/C electrode at various CO partial pressures in 0.5 M H_2SO_4.

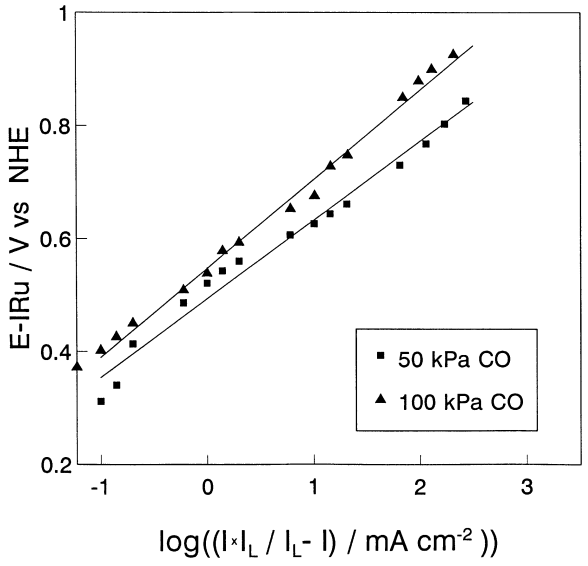

Fig. 8. Ohmic drop and mass-transfer corrected Tafel plots for carbon monoxide oxidation in 0.5 M H_2SO_4 (70 °C) at different CO partial pressures.

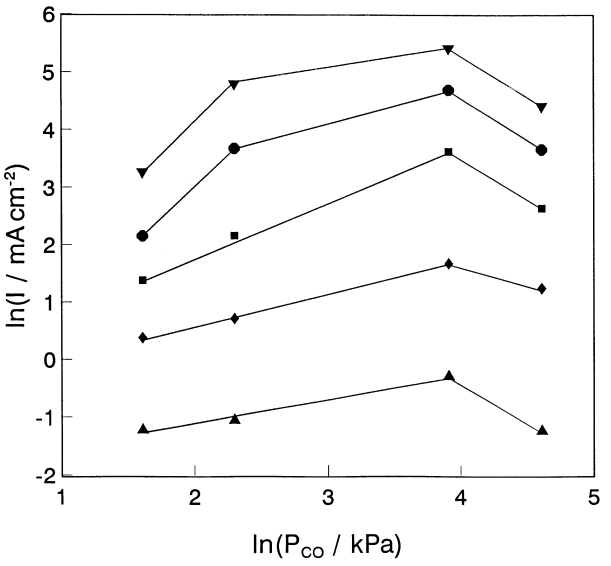

Fig. 10. Dependence of the oxidation current on CO partial pressure at various potentials in 0.5 M H_2SO_4 at 70 °C. Potentials: (▲) 0.5, (◆) 0.6, (■) 0.7, (●) 0.8 and (▼) 0.9 V vs NHE.

The observed activation energy for the electrooxidation of CO at relatively low overpotentials ($\sim 70\,kJ\,mol^{-1}$) is significantly higher than that of a process controlled by surface migration of reacting species; thus, the observed activation energy is likely associated to the formation of the surface complex between CO and OH species [45]. The decrease of activation energy with the increase of overpotential could be related to an increased availability of OH species through the water displacement [16] and/or to the decrease of the adsorption strength between CO and Pt sites due to the formation of Pt-oxide. This latter conjecture seems to be supported by the observed increase of the reaction order with respect to CO with the increase of overpotential.

5. Conclusions

The analysis of the electrochemical oxidation of CO on Pt–Ru/C surfaces has allowed information on the reaction mechanism occurring on gas diffusion electrodes to be obtained. The following conclusions may be drawn:

(i) The r.d.s. appears to involve a surface reaction between CO and OH adsorbed species. This evidence is supported by the observed reaction orders, Tafel slope and activation energy.

(ii) At low overpotentials the influence on the electrochemical rate of OH coverage on the surface seems to be slightly prevailing with respect to CO adsorption. This would account for a labile OH adsorption under such conditions.

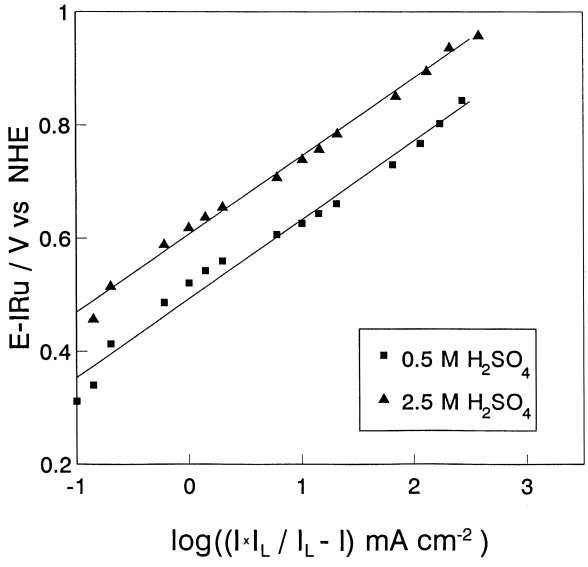

Fig. 9. Ohmic drop and mass-transfer corrected Tafel plots for oxidation of 50 kPa CO in N_2 mixture (70 °C) at different H_2SO_4 concentrations.

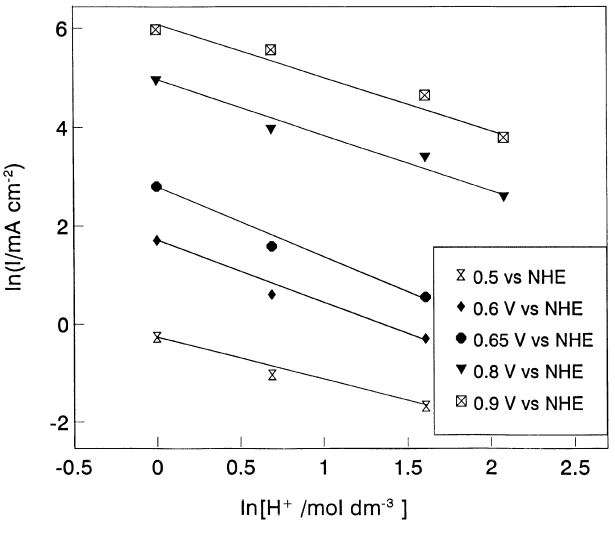

Fig. 11. Dependence of the oxidation current of 50 kPa CO in N_2 mixture on concentration of hydrogen ions at various potentials at 70 °C.

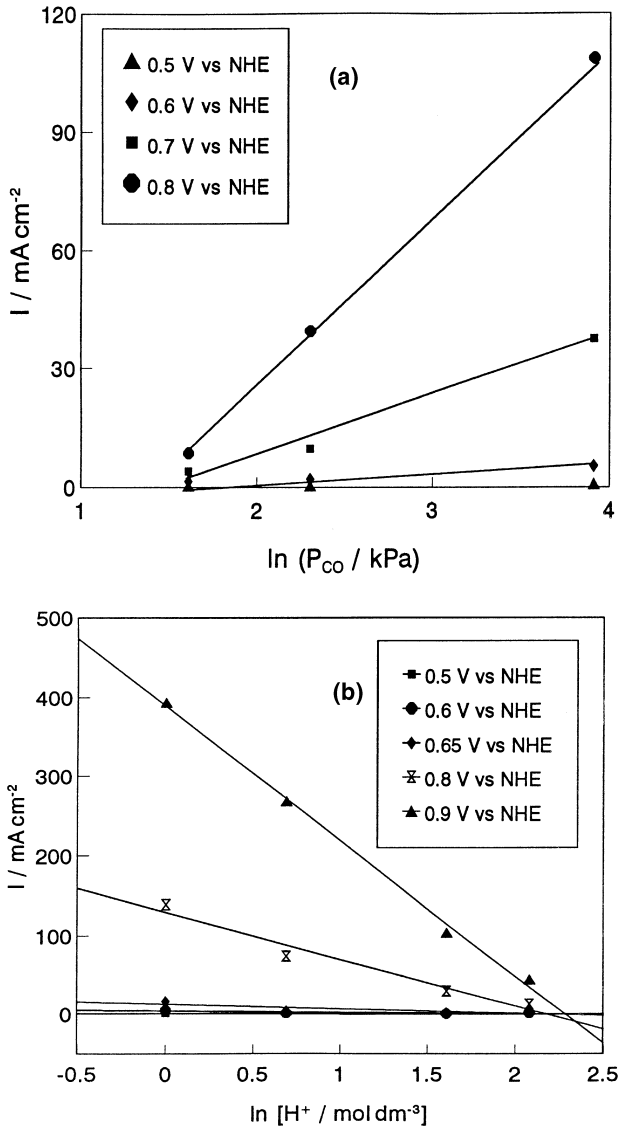

Fig. 12. Dependence of the oxidation current on CO partial pressure (a) and concentration of hydrogen ions for 50 kPa CO in N_2 mixture (b) with respect to the Temkin relationship at various potentials in 0.5 M H_2SO_4 at 70 °C.

(iii) The observed decrease of activation energy with the increase of overpotential would indicate an increased availability of adsorbed OH species on the surface and a faster nucleophilic attack on CO.

(iv) According to the surface properties of the Pt–Ru/C catalyst, the possible interaction of RuO_x species with adsorbed CO molecules on Pt-rich regions is emphasized. This mechanism could occur in parallel to the surface reaction on Pt–Ru pairs in the alloy.

References

[1] K. V. Kordesch and G. R. Simader, *Chem. Rev.* **95** (1995) 191.
[2] H. A. Gasteiger, N. Markovic, P. N. Ross, Jr. and E. J. Cairns, *J. Electrochem. Soc.* **141** (1994) 1795.
[3] R. Parsons and T. VanderNoot, *J. Electroanal. Chem.* **257** (1988) 9.
[4] B. Beden, C. Lamy, N. R. De Tacconi and A. Arvia, *Electrochim. Acta* **35** (1990) 691.
[5] P. A. Christensen, A. Hamnett and G. L. Troughton, *J. Electroanal. Chem.* **362** (1993) 207.
[6] S. Gilman, *J. Phys. Chem.* **66** (1962) 2657.
[7] M. W. Breiter, *J. Electroanal. Chem.* **65** (1975) 623.
[8] P. Stonehart, *Electrochim. Acta* **18** (1973) 63.
[9] P. Stonehart and G. Kohlmayr, *ibid.* **17** (1972) 369.
[10] W. Vogel, J. Lundquist, P. Ross, Jr. and P. Stonehart, *ibid.* **20** (1975) 79.
[11] P. Stonehart and P. Ross, Jr., *ibid.* **21** (1976) 441.
[12] J. M. Leger, B. Beden and C. Lamy, *J. Electroanal. Chem.* **170** (1984) 305.
[13] H. P. Dhar, L. G. Christner, A. K. Kush and H. C. Maru, *J. Electrochem. Soc.* **133** (1986) 1574.
[14] K. Kunimatsu, W. G. Golden, H. Seki and M. R. Philpott, *Langmuir* **1** (1985) 245.
[15] H. P. Dhar, L. G. Christner and A. K. Kush, *J. Electrochem. Soc.* **134** (1987) 3021.
[16] H. A. Gasteiger, N. Markovic, P. N. Ross, Jr. and E. J. Cairns, *J. Phys. Chem.* **98** (1994) 617.
[17] H. A. Gasteiger, N. Markovic and P. N. Ross, Jr., *ibid.* **99** (1995) 8290.
[18] M. Watanabe and S. Motoo, *J. Electroanal. Chem.* **60** (1975) 275.
[19] R. de Levie, *Advances in Electrochemistry and Electrochemical Engineering* **6** (1967) 329.
[20] K. Micka, *Advan. Chem. Ser.* **47** (1965) 73.
[21] S. Srinivasan, H. D. Hurwitz and J. O'M Bockris, *J. Chem. Phys.* **46** (1967) 3108.
[22] L. G. Austin, M. Ariet, R. D. Walker, G. B. Wood and R. H. Comyn, *Ind. Eng. Chem. Fundamentals* **4** (1965) 321.
[23] J. O'M Bockris and B. D. Cahan, *J. Chem. Phys.* **50** (1969) 1307.
[24] R. Kh. Burstein, V. S. Markin, A. G. Pshenichnikov, Yu A. Chismadzhev and Yu G. Chirkov, *Electrochim. Acta* **9** (1964) 773.
[25] J. O'M Bockris and J. O'M Bockris, in 'Fuel Cells. Their Electrochemistry', McGraw-Hill, New York (1969), p. 283.
[26] T. E. Springer and I. D. Raistrick, *in* 'Proceedings of the Symposium on Electrode Materials and Processes for Energy Conversion', Vol. 87–12 (edited by S. Srinivasan, S. Wagner and H. Wroblowa), The Electrochemical Society, Pennington, NY (1987), p. 152.
[27] A. S. Aricò, A. K. Shukla, V. Antonucci and N. Giordano, *J. Power Sources* **50** (1994) 177.
[28] C. D. Wagner, M. W. Riggs, L. E. Davis and J. F. Moulder, *in* 'Handbook of X-ray Photoelectron Spectroscopy', (edited by G. E. Mullemberg), Perkin–Elmer Corporation, Eden Prairie, Minnesota (1978).
[29] B. J. Kennedy and A. W. Smith, *J. Electroanal. Chem.* **293** (1990) 103.
[30] A. S. Aricò, V. Antonucci, N. Giordano, A. K. Shukla, M. K. Ravikumar, A. Roy, S. R. Barman and D. D. Sarma, *J. Power Sources* **50** (1994) 295.
[31] A. K. Shukla, M. K. Ravikumar, A. Roy, S. R. Barman, D. D. Sarma, A. S. Aricò, V. Antonucci, L. Pino and N.Giordano, *J. Electrochem. Soc.* **141** (1994) 1517.
[32] A. S. Aricò, V. Antonucci, V. Alderucci, E. Modica and N. Giordano, *J. Appl. Electrochem.* **23** (1993) 1107.
[33] T. Engel and G. Ertl, *Adv. Catal.* **28** (1979) 1.
[34] A. J. Bard and L. R. Faulkner, *in* 'Electrochemical Methods: Fundamentals and Applications', Wiley, New York (1980), pp. 109–110.
[35] J. H. Hirschenhofer, D. B. Stauffer and R. R. Engleman, *in* 'Fuel Cells, A Handbook (Revision 3)', DOE, Morgantown, West Virginia, (1994), p. 1–13.
[36] H. A. Gasteiger, N. M. Markovic' and P. N. Ross, Jr., *J. Phys. Chem.* **99** (1995) 16757.
[37] V. S. Bagotzky and Yu. B. Vassiliev, *Electrochim. Acta* **12** (1967) 1323.
[38] A. Aramata and M. Masuda, *J. Electrochem. Soc.* **138** (1991) 1949.
[39] R. Inada, K. Shimazu and H. Kita, *J. Electroanal. Chem.* **277** (1990) 315.
[40] R. Ianniello, V. M. Schmidt, U. Stimming, J. Stumper and A. Wallau, *Electrochim. Acta* **39** (1994) 1863.
[41] T. Iwasita, F. C. Nart and W. Vielstich, *Ber. Bunseges. Phys. Chem.* **95** (1991) 638.
[42] C. Gutierez, J. A. Caram and B. Beden, *J. Electroanal. Chem.* **305** (1991) 289.
[43] J. Lu, A. Bewick, *ibid.* **277** (1990) 315.
[44] A. Hamnett, B. J. Kennedy and F. E. Wagner, *J. Catal.* **124** (1990) 30.
[45] P. Shiller and A. B. Anderson, *J. Electroanal. Chem.* **339** (1992) 201.